Ibn Al-Haitham Journal for Pure and Applied Sciences
Journal homepage: jih.uobaghdad.edu.iq
PISSN: 1609-4042, EISSN: 2521-3407
IHJPAS. 2025, 38(2)

Design and Structural Characterization of Novel Azo-Theophylline as Acid-Base Indicator

Mohnned Hamady Manulla[1*] and Alyaa khider Abbas[2]
[1,2]Department of Chemistry, College of Science, University of Baghdad, Baghdad, Iraq.
*Corresponding Author.

Received: 29 June 2023 Accepted: 3 September 2023 Published: 20 April 2025
doi.org/10.30526/38.2.3637

Abstract

Novel heterocyclic acid-base indicators 8-[3-(phenol)azo] theophylline (PAT) and 8[1-(6-sulfonic acid naphthalene) azo] theophylline (SAT) were synthesized through the reaction between m-amino phenol and 1-amino naphthalene -6-sulfonic acid with sodium nitrite to form the diazonium salt at a temperature 0-5˚C in an acidic medium, then a coupling process between the diazonium salt and theophylline compound to produce pigments at the same temperature while maintaining the PH level at 5-6. This study aims to prepare acid-base indicators based on azo dyes. The structural features of these indicators were examined via elemental analyses [FTIR, UV-Vis, and HNMR] spectroscopies, thermal analysis (TGA), and scanning electron microscopy (SEM); the dyes showed good Nanoscale properties. The efficiency of these compounds to act as acid-base indicators has been investigated. This is due to the ability of azo compounds to change their colors in acid and alkaline environments. Compounds SAT and PAT showed good sensitivity towards changing the value of PH, and the color contrast was apparent. The research aims to prepare acid-base indicators based on azo dyes.

Keywords: Acid-base indicator, Azo compound, Structural features, Theophylline, Thermogravimetric analysis.

1. Introduction

Azo dyes are a broad category of synthetic chemical substances (1). They have constantly received attention because they can be used in various fields, such as systems and liquid crystalline devices (2), textile dyes (3,4), biological processes (5).

Azo dyes are colored organic compounds that exhibit outstanding molar absorption coefficients and photochemical and thermal isomerization (6). The existence of a chromophore group and a dye's capacity to absorb electromagnetic radiation in the visible range (400–700 nm) determine its coloring property. Dyes are colored primarily due to their absorption of a particular wavelength of visible light (7). A heterocyclic, autochrome, chromophoric, and solubilizing

group are azo dye's chemical structure components. The ligands' azo function (-N=N-), which exhibits a strong color within the visual range and is sensitive to variations in acidity (pH), makes them useful as indicators in analytical chemistry (8-12). Azo dyes have been widely used as acid-base indicators for the past ten years due to their easy synthesis, stability, high efficiency, and low titration degradability. Additionally, they are occasionally employed to detect the endpoint of strong acids and bases' titrations (13). For instance, Methyl Red turns red below pH 4.4, yellow at pH 6.2, and orange in the middle. Researchers in many domains have used this characteristic extensively since it is conducive to detecting pH levels (14,15). The water solubility of a colorimetric chemosensor is critical for accurate pH estimations in cellular solutions and fluid secretion by the bio-gland (16). As a result, in physiology, a water-soluble, highly pH-sensitive colorimetric chemosensor with a considerable color shift in a weak acid or weak base environment would be extremely valuable (17,18). This study aims to prepare acid-base indicators based on azo dyes.

2. Materials and Methods

2.1. Instruments

The target compounds used chemicals and solvents from Sigma-Aldrich, Fisher, and Merck brands without purification. The MEL-TEMP II equipment was used to record the melting point using the uncorrected open capillary tube method. The FTIR spectra were recognized using FTIR 600. On the (Shimadzu 1800-UV) spectrophotometer, UV-Vis spectra for the examined substances were calculated utilizing distilled water in the zone of (200-1100) nm, scanning electron microscopy (SEM) (Hitachi, Model: S-3400N), 1HNMR spectra were performed by 60,60MHz spectrometer by using DMSO as solvent. The EURO EA 3000 was used to determine the CHNS element analyses (Eure Ea 3000 elemental analyzer), and thermogram analysis (TG) (SDT Q600 V20.9 Build) was used to obtain the thermal analysis (TG).

2.2. Synthesis of indicators (PAT and SAT)

As stated in the literature (19) (0.01 mol, 1.091 g of m-amino phenol, and 0.01 mol, 2.23 g of 1- amino naphthalene -6-sulfonic acid) both separately were dissolved in a solution of (10 mL) Acetic acid and (20 mL) distilled water at 0-5˚C which was diazotized by Using (0.75 g, 0.011 mol) of sodium nitrite dissolved in (10 mL) of distilled water. The end outcome is diazonium salt. The two solutions were combined separately with the coupling agent theophylline (0.01 mol, 1.8016 g) diluted in a 10% alcoholic NaOH solution. After leaving the reaction mixture overnight, the colorful precipitates were filtered, washed with water-ethanol [1:1], dried, and collected, as shown in **Scheme 1**. The physical properties are tabulated in **Table 1**.

Table 1. Physical properties of the two dyes.

Name of dye	Symbol	M.wt (g/mol)	Color	m.p (C^0)	Yield %
8-[3-phenol)azo] theophylline ($C_{13}H_{12}N_6O_3$) (300.29)	PAT	300	Brwn	228 - 230	80
8[1-(6-sulfonic acid naphthalene) azo] theophylline ($C_{17}H_{14}N_6O_5S$) (414.41)	SAT	414	Red	145-147	85

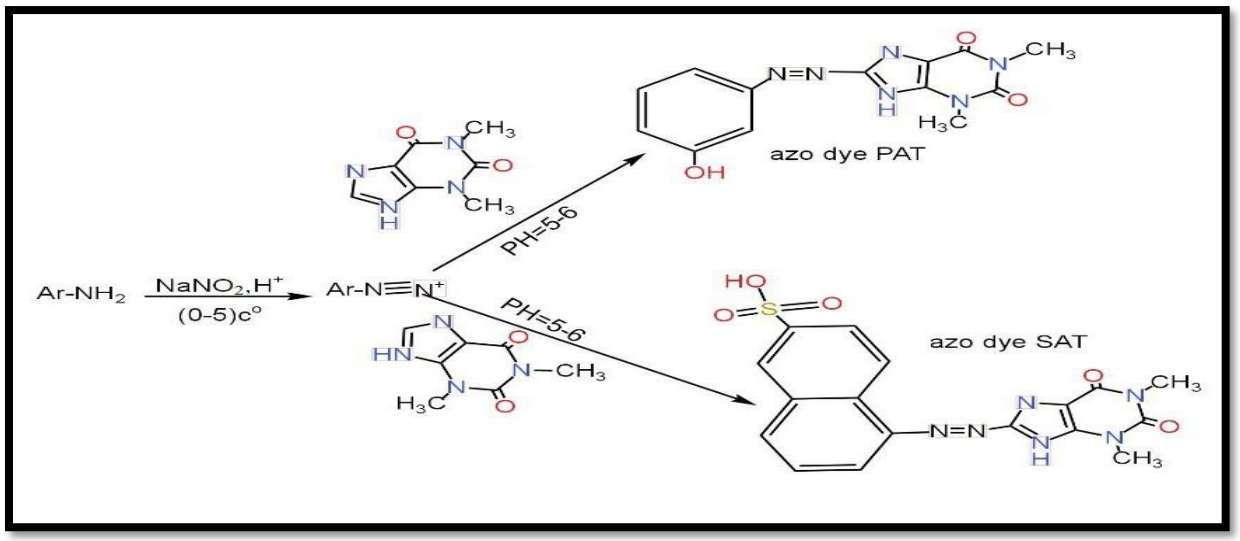

Scheme 1. Synthesis of indicators (PAT) and (SAT); (Ar=NH_2)= m-amino phenol and 1-amino naphthalene-6-sulfonic acid.

3. Results and Discussion

This study synthesized the novel azo indicator PAT and SAT by coupling m-amino phenol and 1-amino naphthalene -6-sulfonic acid with theophylline. In the first step, the diazonium salt is prepared and then reacted as an electrophile with a nucleophile, represented by theophylline. The indicators are stable in air and soluble in water. **Table 2** shows some physicochemical properties.

Table 2. Some data from analytic and physical sources for indicators.

Compounds (M.wt) (gm/mol)	**Color λ (nm)**	**Elemental analysis**			
		C	**H**	**N**	**S**
PAT($C_{13}H_{12}N_6O_3$)	Brown	52.2	3.4	27.2	-----
(300.29)	436	51.9	3.9	27.9	
SAT($C_{17}H_{14}N_6O_5S$)	Red	49.6	3.7	20.41	8.1
(414.41)	514	49.22	3.37	22.26	7.7

3.1. Thermogravimetric analysis (TGA)

TGA assays showed that the indicator SAT and PAT are thermally degradable at (25-1000)^oC in argon gas. **Table 3** limited the mass loss, stages of decomposed parts, and TG range of the decomposition, as displayed in **Figures 1** and **2**. The proposed formula and thermal stability were validated using thermal analysis for the synthesized indicators (PAT and SAT). Deduce that the PAT is more thermally stable than SAT from the (TGA) curves due to the residues of SAT (22%) and PAT (46.54%) being the same.

Table 3. The TGA of PAT and SAT.

Com. Sym Chemical Formula	Steps	TG. Range of the decomposition(°C)	Suggested assignment	%Mass loss Calculated %	%Mass loss Found %
PAT ($C_{13}H_{12}N_6O_3$)	1	25-165	C_2H_{12}	11.98	11.80
	2	165 -380	C_{25}	9.99	10.01
	3	380-850	$C_{6.5}$	25.97	26.50
	4	849-1000	$C_{1.25}$	4.99	5.02
	5	Residue	$C_{0.75}N_6O_3$	46.54	46.54
SAT ($C_{17}H_{14}N_6O_5S$)	1	25 – 200	C_4H_2	12.06	12.07
	2	200 -390	C_8H_{12}	26.06	26.24
	3	390 – 540	$C_{3.25}$	9.41	9.79
	4	540 -950	$C_{1.75}N6O_{1.5}$	31.1	30.98
	5	Residue	$O_{3.5}S$	21.1	20.91

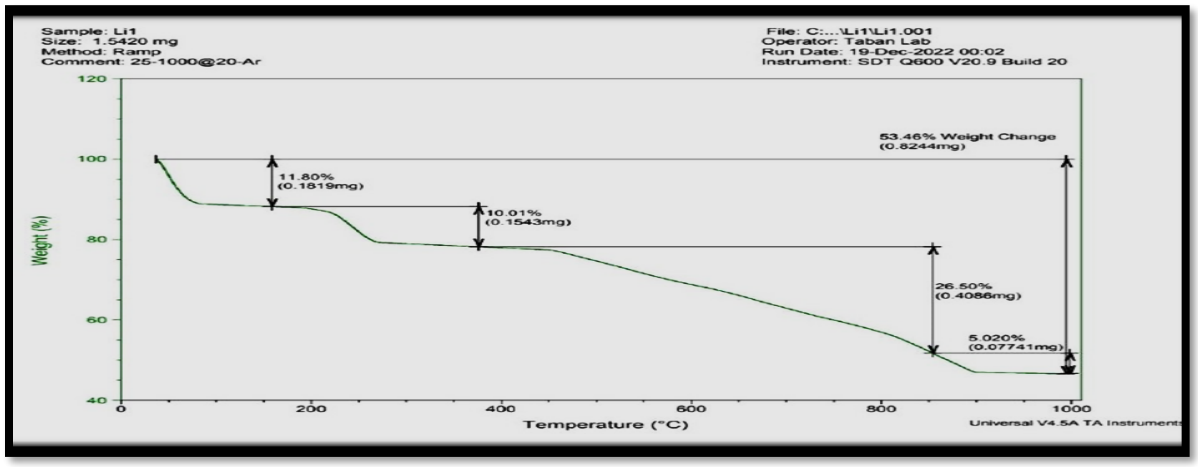

Figure 1. TG-thermogram of (PAT) indicator.

3.2. Fourier transform infrared spectra of the compounds (FT-IR)

The FT-IR spectrum of the indicator (PAT) in **Figure 3** showed the main bands were discovered at (3433, 1701, 1639, 1575, 1421, 1334) cm^{-1} assigned to υ(N-H), υ(C=O), υ(C=N), υ (C-N=N-C), υ(N=N), υ(N-H) [20].While the same extended vibration modes ranges of the indicator (SAT) in **Figure 4** appeared at (1224, 1417, 1440, 1560, 1666, 1641, 1710, 3440, and 3380) cm^{-1}, as well as the band at (1224) cm^{-1}, which was attributed to υ (SO_3H), as shown in **Table 4**.

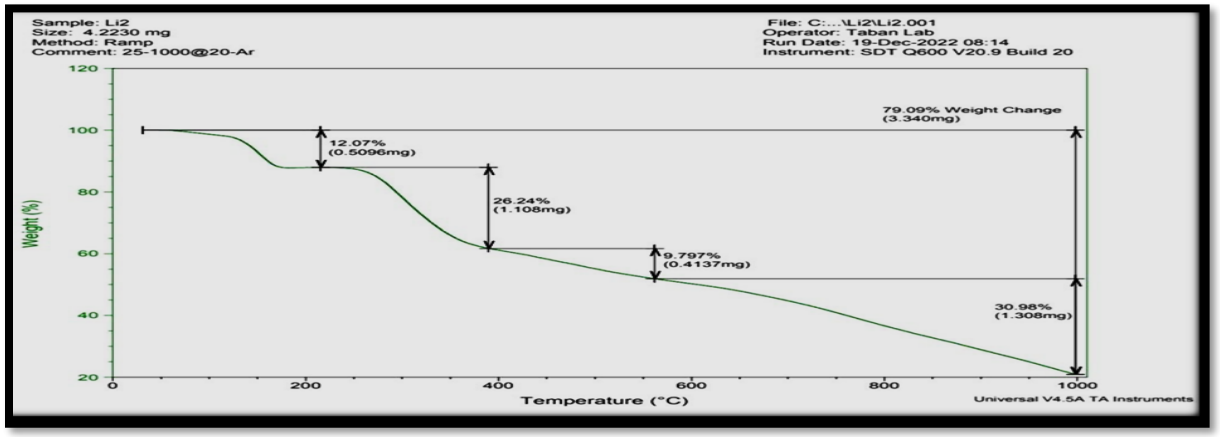

Figure 2. TG-thermogram of (SAT) indicator.

Table 4. The FTIR assignments for PAT and SAT indicators.

Compound	υ(OH) υ(N-H)	υ (C=O)	υ (C=N)	υ (C=C)	υ (N=N)	υ (-CN=NC-)	υ (SO_3H)
PAT	3433 st 3288 m	1701 vw	1641 d,st	1558st	1413 m	1338w	
SAT	3440 3425 d,st 3288 m	1710 m	1666 1641 dm	1560st	1417 sh	1483w	1224 sh

Sh=sharp, m=medium, w=weak, d=doublet, vw=very weak.

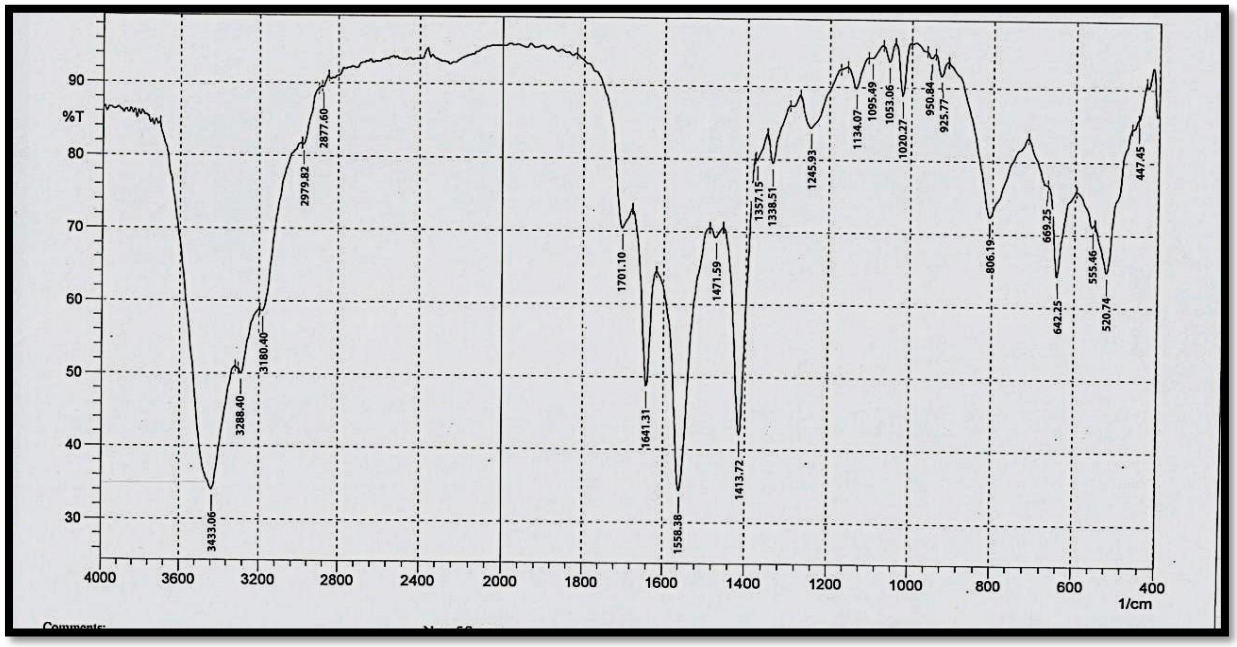

Figure 3. The FTIR spectrum of PAT.

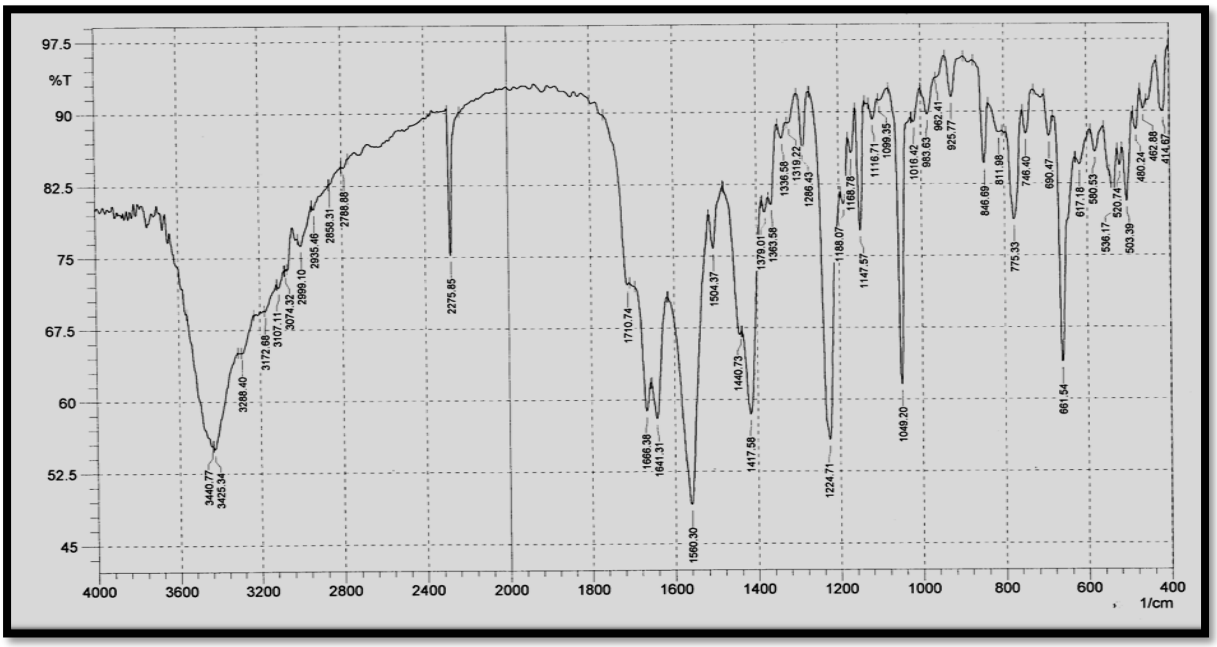

Figure 4. The FTIR spectrum of SAT.

3.3. The ^{1}HNMR of indicators

The generated indicators' ^{1}HNMR spectra were compared using TMS as an internal standard, and chemical shift data (δ) in ppm for various proton types are shown in **Figures 5** and **6**. The ^{1}HNMR spectra were captured in the DMSO-d6 solution, while all data are shown in **Table 5**. A single signal appeared at (14.5 and 13.75) ppm belonging to (N-H, H) in the imidazole moiety in theophylline for PAT and SAT, respectively (21).

Two signals are shown by the free ligand (PAT) at (3.36 and 3.48) ppm can be attributed to the protons of (N-CH_3pyrm) ppm and a singlet signal at (6.75) ppm belong to (OH, H) of phenol moiety. The multiple signals at (6.74- 6.67) ppm which related to benzene ring (22), as well as the ligand (SAT) displayed two singlet signales at (3.44 and 3.24) ppm attvibuted to (N-CH_3) at pyrimidine moiety. At the same time, the SO_3H have asignal at (8.04) ppm (23). The naphthalene multiple signals at (7.38-8.40) ppm (12). DMSO and H_2O were connected to the singlet signals at (1.8 and 3.5) ppm, respectively.

Table 5. The chemical shift [δppm] of SAT and PAT ligands.

Compound	N-CH_3 pyrm.	N-H imd	Ar-H	OH δppm	SO_3H δppm	Naph.
PAT	3.36 3.48	14.5	6.74-667	6.75	-	
SAT	3.44 3.94	13.75	-	-	8.04	7.38-8.40

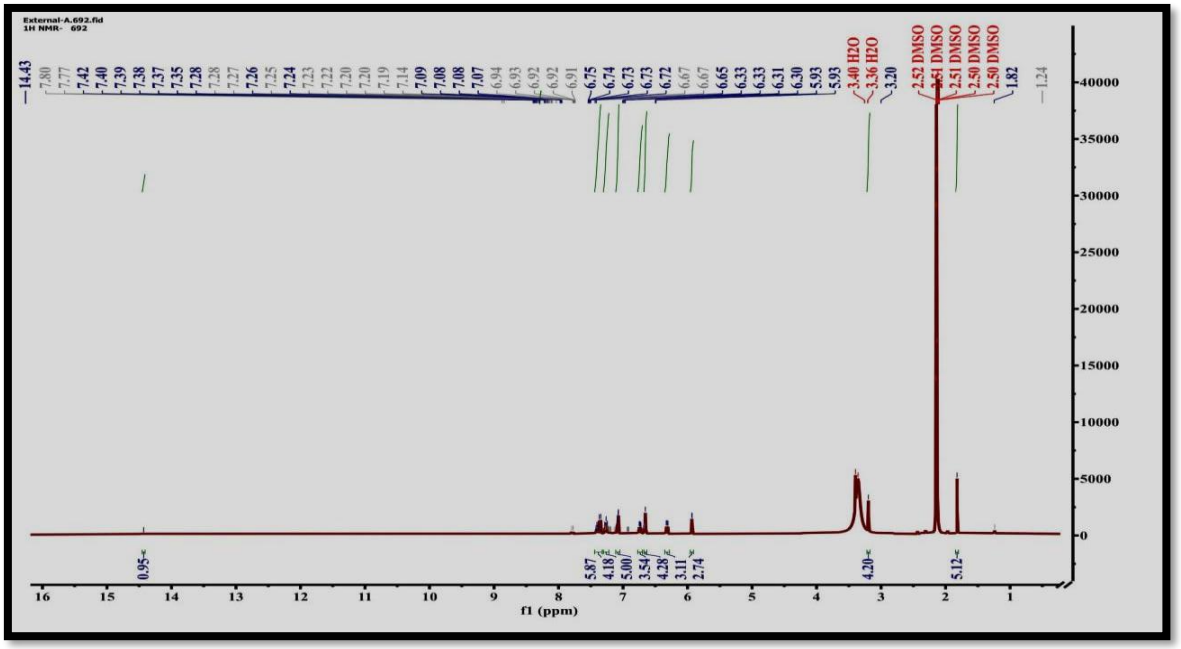

Figure 5. The ^{1}HNMR Spectrum for the (PAT).

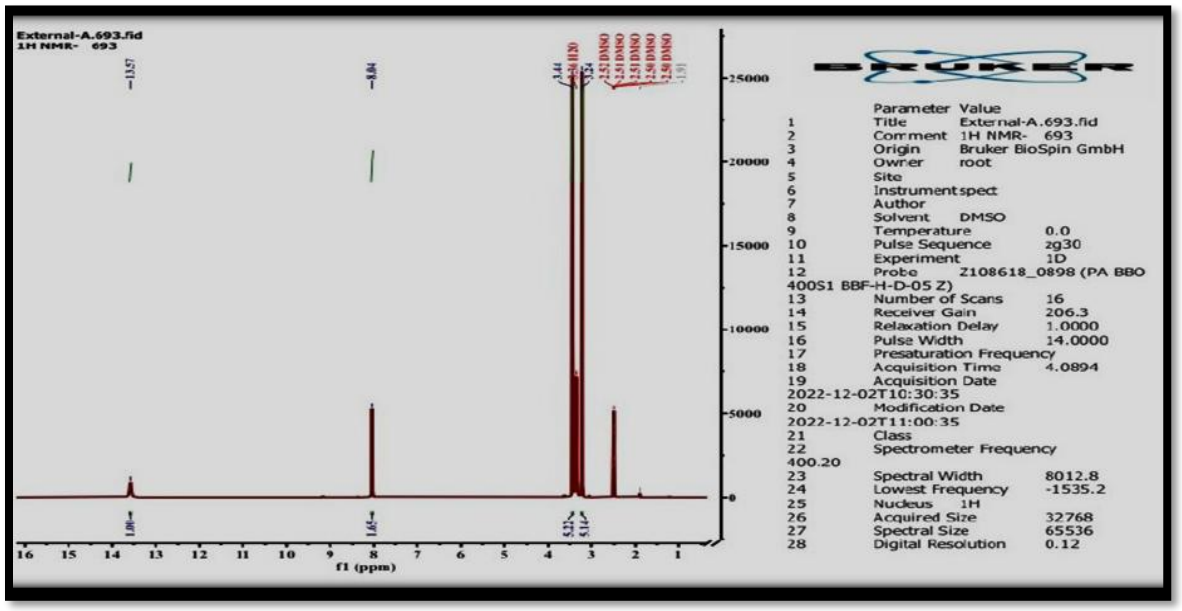

Figure 6. The ^{1}HNMR Spectrum for the (SAT).

3.4. The UV-Vis spectra

It is one of the methods for characterizing compounds that are most frequently utilized (UV-Vis). The (PAT and SAT) were examined at a concentration of (10^{-3} M) using water as a solvent with a range (190-1100 nm). The acquired results are presented in **Table 6**, and the electronic spectra are displayed in **Figures 7** and **8**. Two bands may be seen in the electronic spectrum of the (PAT) at (436 nm, 22935 cm^{-1}), and (286 nm, 370 37 cm^{-1}). The first band represents the energy of the intramolecular charge transfer (INCT) through azo linkage (24,25). Moreover, the pyrimidine intramolecular transition [inter CT], imidazole, and benzene moieties were found in the UV area ($\pi\rightarrow\pi^*$) transition (26). The ligands (SAT) appeared at four peaks. At (370 nm, 27027cm^{-1}) and (514 nm,19455 cm^{-1}) back to electronic transition ($n\rightarrow\pi^*$),while the bands at (244 nm, 40983 cm^{-1}) and (339 nm, 29498 cm^{-1}) were related to ($\pi\rightarrow\pi^*$) transition (26).

Table 6. Electronic transitions, of the indicators at (10^{-3} M).

Compound (Color in solution)	Wave length (nm)	Wave number (cm^{-1})	Assignment
PAT	436	22935	$n\rightarrow\pi^*$
Dark orange	286	34965	$\pi\rightarrow\pi^*$
SAT .	514	19455	$n\rightarrow\pi^*$
Red	370	27027	$n\rightarrow\pi^*$
	339	29498	$\pi\rightarrow\pi^*$
	244	40983	$\pi\rightarrow\pi^*$
	217	46.082	$\pi\rightarrow\pi^*$

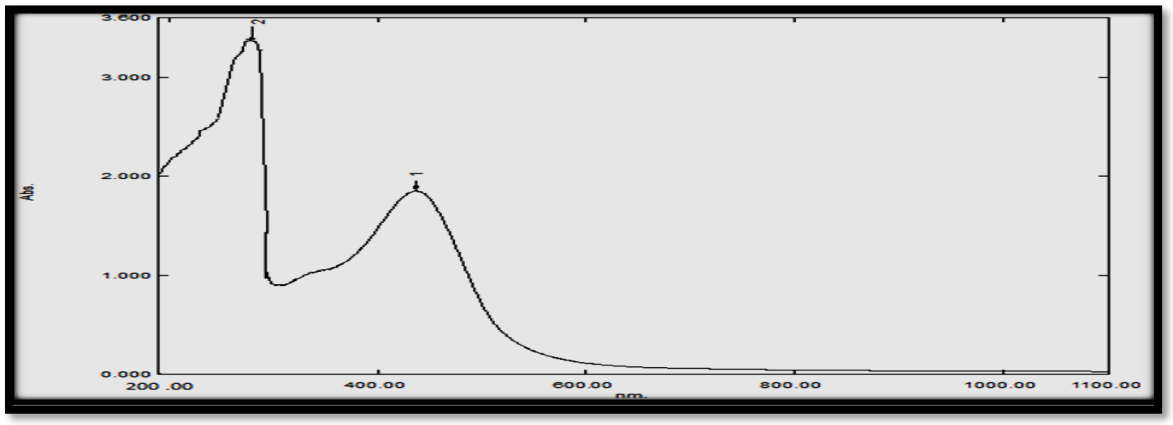

Figure 7. The UV-Vis Spectrum for the PAT.

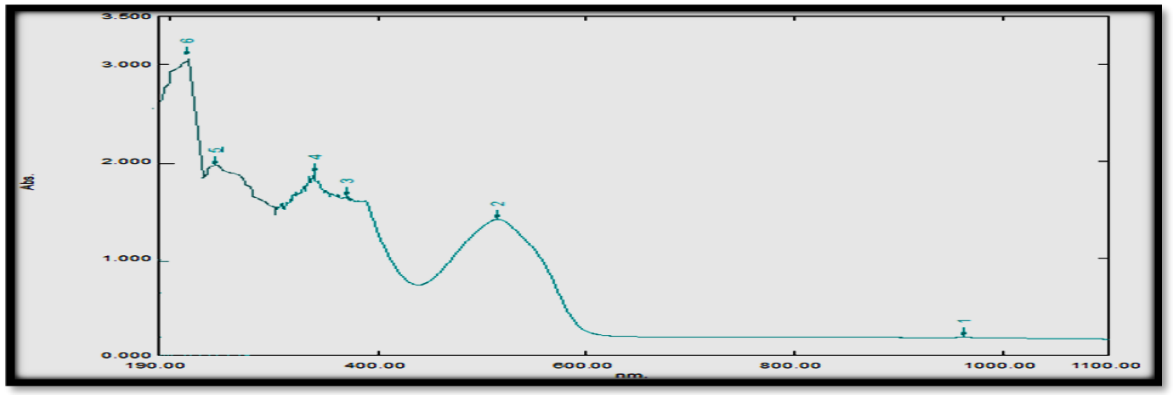

Figure 8. The UV-Vis Spectrum for the SAT.

3.5. Scanning electron microscopy analysis (SEM)

For the characterization of 2D and 3D materials, SEM is a highly flexible method. The SEM has excellent spatial resolution in imaging and chemical characterization modes, from nano- to microscale (28). Different crystalline structures and surface homogeneities may be seen in the morphology of the (SAT and PAT) who attended, as mentioned in the practical part. SEM procedure was accredited for a cross section's area (100 nm) and expanding power (Mag=20.00KX and 50.00 KX) as displayed in **Figures 9** and **10**, respectively. The SEM pictures demonstrated heterogeneous surfaces with various forms that vary with multiple compounds and particle volume changes **Table 7**.

Table 7. Morphological surface of the (PAT and SAT) compounds.

Compound	Average volume (nm)	Shape
PAT	133.6	sheets
SAT	53.65	corale

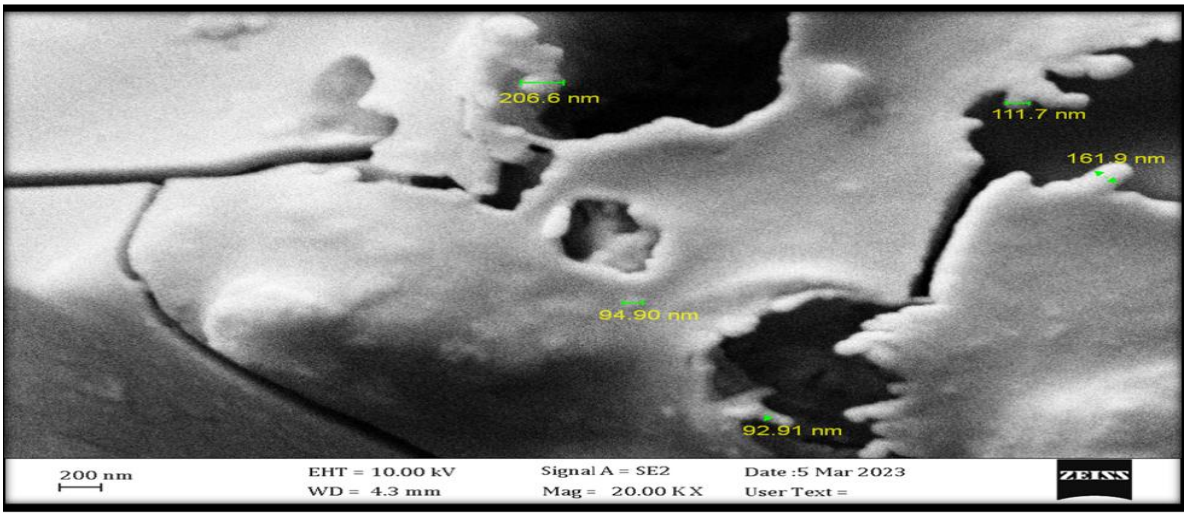

Figure 9. The SEM analysis for the [PAT].

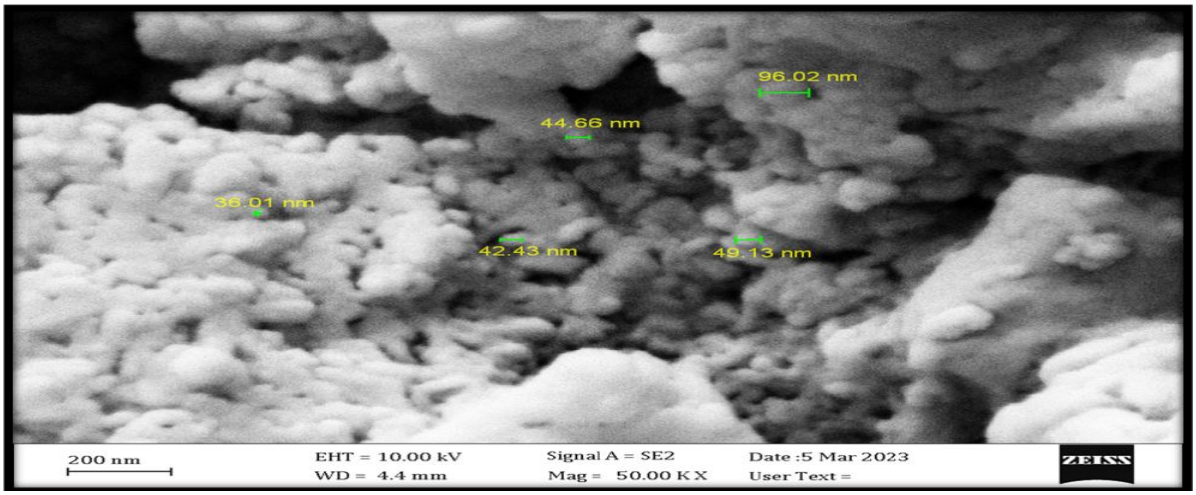

Figure 10. The SEM analysis for the [SAT].

3.6. Acid-base indicator

Azo dyes have been widely used as acid-base indicators for the past ten years due to their easy synthesis, stability, high efficiency, and low titration degradability (29,30).

In acid-base titration, the (PAT and SAT) were used as indicators by utilizing (0.1 M) of HCl against (0.1 M) NaOH and (0.1 M) of CH_3COOH against (0.1 M) of NaOH. The indicators are evident in either an acidic or basic solution. They exhibit a good color change when transitioning between the two, as shown in **Figures 11** and **12**. All data was collected in **Tables 8** and **9**.

Table 8. Titration of acid (0.1 M) against NaOH (0.1 M) for (PAT).

NO	Volume	Volume of NaOH	Color with acid	Color with base
1	(HCl) 5 mL	2 mL	Deep orange	Light orange
2	(ACOH) 5 mL	6 mL	Red	light orange

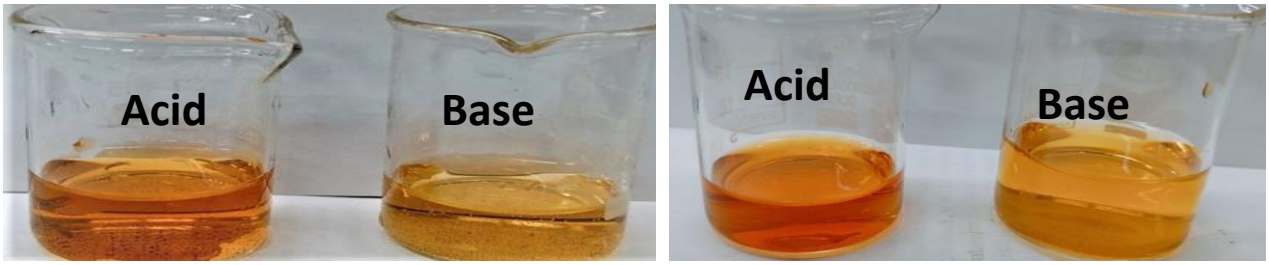

PAT with HCl **PAT with CH_3COOH**

Figure 11. Change in color of Azo indicator (PAT) in acid and base solutions.

Table 9. Titration of acid (0.1 M) against NaOH (0.1 M) for (SAT).

NO	Volume	Volume of NaOH (mL)	Color with acid	Color with base
1	HCl: 5	3	Red	Light yellow
2	ACOH: 5	4	Pink	Yellow

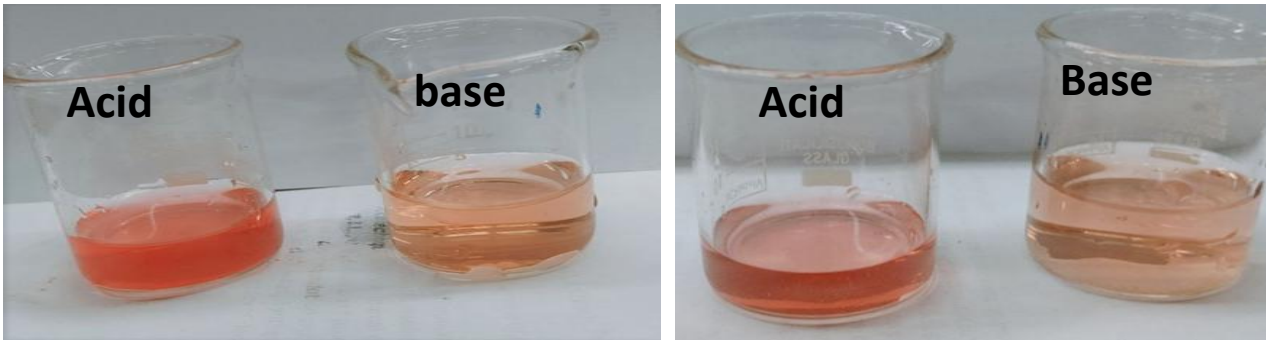

SAT with HCl **SAT with CH_3COOH**

Figure 12. Change in color of Azo indicator (SAT) in acid and base solutions.

4. Conclusion

The ability of the synthesized novel azo compounds (PAT and SAT) to work as acid-base indicators was investigated by different acid-base titrations.Using acid-base titrations between (NaOH, HCl) and (NaOH, CH_3COOH), the capacity of the produced azo compounds to serve as acid-base indicators were examined. Each azo compound accurately identified the endpoint. As well as the formula was detected by various physiochemical methods.

Acknowledgments

The authors thank the Department of Chemistry/ College of Science/ University of Baghdad for their support.

Conflict of Interest

The authors declare that they have no conflicts of interest.

Funding

Department of Chemistry at the College of Science/ University of Baghdad supported this work.

Ethical Clearance

This study was approved by the Scientific Committee at the Department of Chemistry/ College of Science/ University of Baghdad.

References

1. Radulescu-Grad ME, Visa A, Milea MS, Lazău RL, Popa S, Funar-Timofei S. Synthesis, spectral characterization, and theoretical investigations of a new azo-stilbene dye for acrylic resins. J Mol Struct. 2020; 1217(6):128380. https://doi.org/10.1016/j.molstruc.2020.128380.
2. Mallikarjuna N, Keshavayya J. Synthesis, spectroscopic characterization and pharmacological studies on novel sulfamethaxazole based azo dyes. J King Saud Univ Sci. 2020; 32(1):251-259. https://doi.org/10.1016/j.jksus.2018.04.033.
3. Tasli PT, Atay ÇK, Demirturk T, Tilki T. Experimental and computational studies of newly synthesized azo dyes based materials. J Mol Struct. 2020; 1201:127098. https://doi.org/10.1016/j.molstruc.2019.127098.
4. Bideau FL, Mohamed-Smati SB, Faraj FL, Becheker l, Berredjem H, Bideau FL, Hamdi M, Rachedi DY. Synthesis, characterization and antimicrobial activity of some new azo dyes derived from 4-hydroxy-6-methyl-2H-pyran-2-one and its dihydro derivative. Dyes Pigm. 2021; 188(4):109073. https://doi.org/10.1016/j.dyepig.2020.109073.
5. Aboudan M, Kassab R. Synthesis of new azo dyes derived from 2,7-dihydroxynaphthalene. Int J Acad Res. 2015; 3(4):143-149. http://www.ijasrjournal.org/.
6. Manjunatha B, Bodke YD, Nagaraja O, Lohith TN, Nagaraju G, Sridhar MA. Coumarin-benzothiazole based azo dyes: synthesis, characterization, computational, photophysical and biological studies. J Mol Struct. 2021; 1246:131170. https://doi.org/10.1016/j.molstruc.2021.131170.
7. Alsantali RI, Raja QA, Alzahrani AYA, Sadiq A, Naeem A, Mughal EU, Al-Rooqi MM, El Guesmi N, Moussa Z, Ahmed SA. Miscellaneous azo dyes: A comprehensive review on recent advancements in biological and industrial applications. Dyes Pigm. 2022; 199:110050.
8. Mohammed H. Synthesis, identification, and biological study for some complexes of azo dye having theophylline. Sci World J. 2021; 2021(9943763):231-243. https://doi.org/10.1155/2021/9943763.
9. Chung KT. The significance of azo-reduction in the mutagenesis and carcinogenesis of azo dyes. Mutat Res. 1983; 114(3):269-281. https://doi.org/10.1016/0165-1110(83)90035-0.
10. 10. MacKenzie K, O'leary B. Inorganic polymers (geopolymers) containing acid–base indicators as possible colour-change humidity indicators. Mater Lett. 2009; 63(2):230-232. https://doi.org/10.1016/j.matlet.2008.09.053.
11. Prasad KK, Raheem S, Vijayalekshmi B, Sastri CK. Basic aspects and applications of tristimulus colorimetry. Talanta. 1996; 43(8):1187-1206. https://doi.org/10.1016/0039-9140(96)01871-1.
12. Al-Majidi. S.M; Al-Khuzaie. M.G. Synthesis and characterization of new azo compounds linked to 1, 8-naphthalimide and studying their ability as acid-base indicators. IJS. 2019; 5(2):2341-2352. https://doi.org/10.24996/ijs.2019.60.11.4.
13. Naime J, Al Mamun MS, Aly MAS, Karim KMR, Maniruzzaman M, Badal MMR. Synthesis, characterization and application of a novel polyazo dye as a universal acid–base indicator. RSC Advances. 2022; 12(43):28034-28042. https://doi.org/10.1039/D2RA04930A.
14. Bishop E. Indicators: International series of monographs in analytical chemistry. 2013; 51(2):1-40.
15. Kahlert.H; Meyer G; Albrecht.A. Colour maps of acid–base titrations with colour indicators: how to choose the appropriate indicator and how to estimate the systematic titration errors. ChemTexts. 2016; 2(7):1-28. https://doi.org/10.1007/s40828-016-0026-4.
16. Benkhaya S, M'rabet S, El Harfi A. Classifications, properties, recent synthesis and applications of azo dyes. Heliyon. 2020; 6(1):e03271. https://doi.org/10.1016/j.heliyon.2020.e03271.

17. Xie K, Gao A, Li C, Li M. Highly water-soluble and pH-sensitive colorimetric sensors based on a D–π–A heterocyclic azo chromosphere. Sensors Actuators B Chem. 2014; 204:167-174. https://doi.org/10.1016/j.snb.2014.07.090.
18. Mezgebe K and Mulugeta E. Synthesis and pharmacological activities of azo dye derivatives incorporating heterocyclic scaffolds: A review. RSC Advances. 2022; 12(40):25932-25946. https://doi.org/10.1039/D2RA04934A.
19. Jasim DJ, Abbas A. Divalent metal complexes of azosulfamethaxazole: synthesis and characterization with study some of their applications. Nat Volatiles & Essent Oils. 2021; 8(4):8272-8300.
20. Jasim MN. Synthesis, characterization of poly heterocyclic compounds, and effect on cancer cell (Hep-2) in vitro. Baghdad Sci J. 2018; 15(5):456-468. https://doi.org/10.21123/bsj.2018.15.4.0415.
21. Saad HAR, Shakir RM, Mahdi MH. Synthesis and thermal electo conductivity of some new triazole derivatives bearing azo or azomethain group. IHJPAS. 2018; 31(3):88-101. https://doi.org/10.30526/31.3.2018.
22. Abass BF, Musa TMA-D, Aljibouri MN. Preparation and spectroscopic studies of cadmium (II), zinc (II), mercury (II) and vanadium (IV) chelates azo ligand derived from 4-methyl-7-hydroxycoumarin. Indones J Chem. 2021; 21(4):912-919. https://doi.org/10.22146/ijc.63032.
23. Dabish RAA. Synthesis and spectral studies of some new complexes containing azo ligand with anticancer, antibacterial and dyeing performance. Annals of R.S.C.B. 2021; 25(4):7968-8006. http://annalsofrscb.ro.
24. Jasim DJ, Abbas AK. Synthesis, identification, antibacterial, medical and dying performance studies for azo-sulfamethoxazole metal complexes. Eurasian Chem Commun. 2022; 4(1):16-40. https://doi.org/10.22034/ecc.2022.310593.1251.
25. Manulla MH and Abbas AK. La (III) and Ce (IV) complexes of novel azo-theophylline ligand: structural analysis and biological effectiveness. IJS. 2025; 66(1):39-51. https://doi.org/10.24996/ijs.2025.66.1.4.
26. Al-Adilee KJ, Jawad SH, AKadhim H. Synthesis, characterization, biological applications, and molecular docking studies of some transition metal complexes with azo dye ligand derived from 5-methyl imidazole. J Mol Struct. 2024; 1295:136695. https://doi.org/10.1016/j.molstruc.2023.136695.
27. MenY, Le P, Zhou J, Cheng G, Chen S, Luo W. Tailoring the electronic structure of Co_2P by N doping for boosting hydrogen evolution reaction at all pH values. ACS Catalysis. 2019; 9(4):3744-3752. https://doi.org/10.1021/ACSCATAL.9B00407.
28. Inkson BJ. Scanning electron microscopy (SEM) and transmission electron microscopy (TEM) for materials characterization. In book: Materials characterization using nondestructive evaluation (NDE) methods. Elsevier. 2016; p. 17-43.
29. El-Dossoki FI, Abdolla NS, and El-Seify FA. Development of a novel category of azo dyes based on coumarin and metal complexes for potential applications as an acid–base titration indicator and a carbon steel corrosion inhibitor in acidic conditions. Chem Afr. 2024; 7(7):257-272. https://doi.org/10.1007/s42250-023-00722-3.
30. AL-Qaysi WW and Abbas AK. Novel nano Zn^{+2}-compound from LA ligand as an acid-base indicator: Synthesis, characterization, pH sensor, and fluorescent study. IJS. 2023; 22(2):5525-5540. https://doi.org/10.24996/ijs.2023.64.11.6.